Available online at www.sciencedirect.com
SCIENCE DIRECT®

Journal of the European Ceramic Society 24 (2004) 2193–2201

www.elsevier.com/locate/jeurceramsoc

On the description of indentation size effect in hardness testing for ceramics: Analysis of the nanoindentation data

Zhijian Peng, Jianghong Gong*, Hezhuo Miao

Department of Materials Science and Engineering, Tsinghua University, Beijing 100084, PR China

Received 5 January 2003; received in revised form 16 June 2003; accepted 6 July 2003

Abstract

The nanoindentation hardnesses of a commercially available soda-lime glass, a tetragonal ZrO_2 polycrystalline and a hot-pressed Si_3N_4 were measured in the peak load range from 7.5 to 500 mN. The experimental results revealed that, for each material, the measured hardness exhibits a peak-load- dependence, i.e., indentation size effect (ISE). Such a peak-load-dependence was then analyzed using the Meyer' law, the Hay–Kendall approach, the proportional specimen resistance (PSR) model, the elastic recovery model and the modified PSR model. The analyses revealed that: (1) Meyer's law provides a satisfactory description for the experimental data for each material but cannot provide any knowledge of the origin of the observed ISE; (2) the Hays–Kendall approach, the elastic recovery model and the PSR model yield meaningless values of the parameters included in the corresponding equations, invalidating the applicability of these models in analyzing the ISE in the nanoindentation region; (3) the modified PSR model is sufficient for describing the observed ISE but the physical meaning of this model seems to be more complex than those proposed originally. For each material, the true hardness was also determined based on the PSR model, the elastic recovery model and the modified PSR model, respectively. It was found that the true hardness values deduced based on different models are similar with each other and this similarity was attributed to the similarity between the empirical equations adopted in these models.

Keywords: Hardness; Mechanical properties; Nanoindentation

1. Introduction

It is well known that the apparent hardness of a solid, which is usually defined as the ratio of the applied test load to the resulting indentation area, depends on the applied test load.[1–3] This phenomenon, known as the indentation size effect (ISE), usually involves a decrease in the measured apparent hardness with increasing applied test load, i.e., with increasing indentation size. The existence of ISE means that, if hardness is used as a material selection criterion, it is clearly insufficient to quote a single hardness number. There has been voluminous literature devoted to study the origin of the ISE. Consequently, several empirical or semi-empirical equations, including the Meyer's law,[1,2] the Hays–Kendall approach,[4] the elastic recovery model,[5] the energy-balance approach.[6,7] the proportional specimen resistance model,[8] etc., were proposed for describing the variation of the indentation size with the applied test load. Except the Meyer's law, the other approaches all involve the determination of a so-called true-hardness, i.e., a load-independent hardness number. These equations have been widely employed to describe the indentation data obtained for various materials and several studies[8–12] have been conducted to make comprehensive comparisons between these equations. However, all the previously reported work focused mainly on the analyses of the micro- or macro-hardness data and little effort has been devoted to examine the applicability of these empirical or semi-empirical equations to the nanoindentation data. Therefore, the aim of this paper is to report some experimental data on the nanoindentation hardness of glass and ceramics and then to critically examine the observed ISE based on various approaches and models proposed in the literature.

* Corresponding author. Tel.: +86-106-277-2855; fax: +86-106-277-1160.
E-mail address: gong@mse.tsinghua.edu.cn (J. Gong).

0955-2219/$ - see front matter © 2003 Elsevier Ltd. All rights reserved.
doi:10.1016/S0955-2219(03)00641-1

2. Experimental

The materials chosen for this study include a commercially available soda-lime glass, a sintered 3 mol% Y_2O_3 stabilized tetragonal ZrO_2 polycrystalline (TZP) and a hot-pressed (HP) Si_3N_4. The two ceramic specimens, TZP and Si_3N_4, were received with machined surfaces. With these materials the machining- induced surface damages were removed mechanically by polishing, ultimately with 0.5 μm diamond paste, to produce an optical finish. The glass specimen needed no such preparation, for its surface is mirror smooth as a result of the fabrication history. All specimens were in slab form with flat, parallel surfaces.

The nanoindentation tests were conducted with a Berkovich indenter using a fully calibrated Nano Indenter XP (Nanoinstruments Innovation Center, MTS systems, TN, USA). In each test run, the indenter was driven into the specimen surface (loading half-cycle) under a load gradually increased to the predetermined peak value, unloaded gradually to 10% of the peak load (unloading half-cycle) after being held at peak load for 30 s, and then driven again into the specimen surface to a higher value of the peak load. Such a procedure repeated for seven times with increasing peak loads and resulted in a load–displacement curve containing seven loading/unloading cycles. For TZP and glass, five load–displacement curves were recorded while for Si_3N_4 four load–displacement curves were recorded.

3. Results

The load–displacement curves obtained for various materials are shown in Fig. 1. For each material, all the data points of four or five measurements are given in this plot. For soda-lime glass, the load- displacement curves from all the five measurements overlap with each other, indicating a high level of reproducibility. For TZP and Si_3N_4 ceramics, slight scatters exist among the different load–displacement curves. These scatters may be attributed to the intrinsic microstructural inhomogeneity of these two polycrystalline ceramics.

Similar to the conventional microhardness testing, the nanoindentation hardness is usually defined as the ratio of the peak indentation load, P_{max}, to the project area of the hardness impression, A_c, i.e.,

$$H = \frac{P_{max}}{A_c} = \frac{P_{max}}{24.5h_c^2} \quad (1)$$

Different approaches for deducing the contact depth, h_c, from the resultant load–displacement curve have been proposed and perhaps the most widely used one is that of Oliver and Pharr.[13] The Oliver–Pharr data

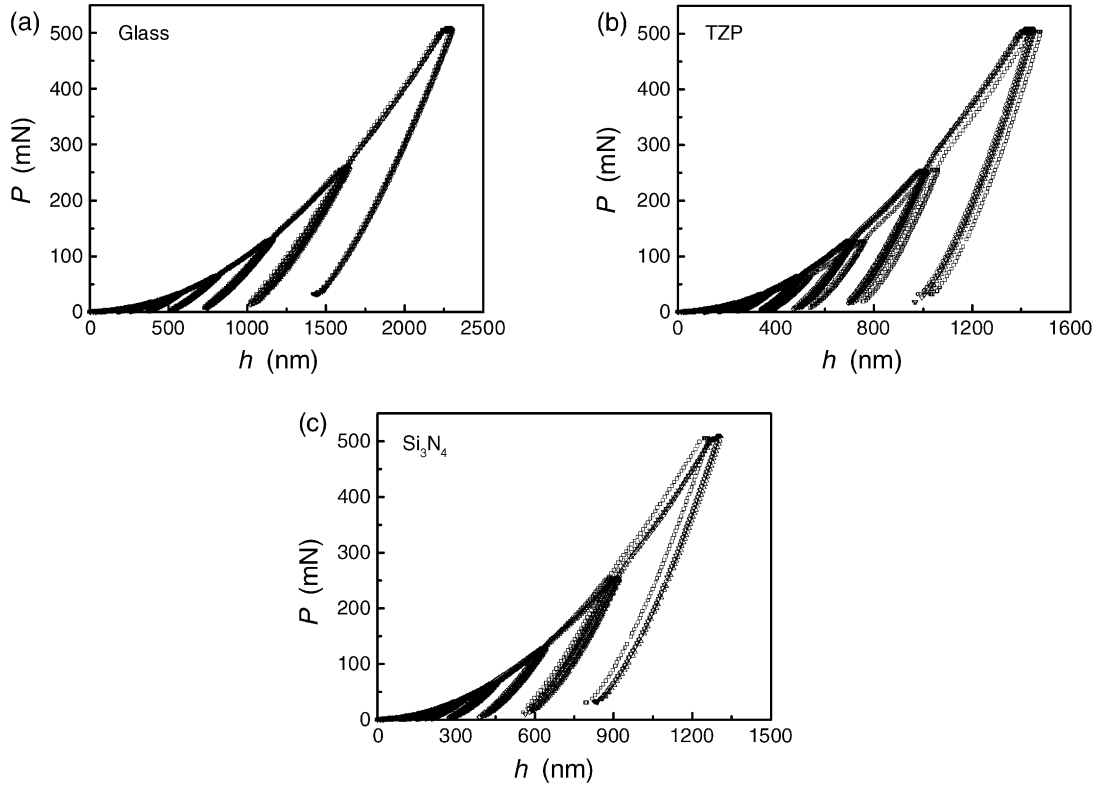

Fig. 1. Load–displacement curves for the test materials. For each material, all data points of the four or five curves are given to show the reproducibility of the measurements.

analysis procedure begins by fitting the unloading curve to an empirical power–law relation[13]

$$P = \alpha(h - h_f)^m \quad (2)$$

where P is the indentation load, h is the indenter displacement, α and m are empirically determined fitting parameters, and h_f is the final displacement after complete unloading and also determined by curve fitting. Once the parameters α, m and h_f are obtained by curve fitting, the initial unloading stiffness, S, can be established by differentiating Eq. (2) at the maximum depth of penetration, $h = h_{max}$. Then the contact depth, h_c, is estimated from the load–displacement data using

$$h_c = h_{max} - \beta\frac{P_{max}}{S} \quad (3)$$

where P_{max} is the peak indentation load and β is a constant dependent on the indenter geometry. For the generally employed Berkovich indenter, it has been shown that β has an empirical value of 0.75.[13]

Fig. 2 shows the experimentally determined nanoindentation hardness, H, as functions of the peak load, P_{max}, for the test materials. Each of the data points represents an average of measurements from four or five tests. For Si_3N_4 and TZP, the apparent hardness decreases with increasing peak load and exhibits a typical indentation size effect. For soda-lime glass, the ISE seems to be less significant.

4. Data analyses

4.1. Meyer's law

The most widely used empirical equation for describing the ISE is the Meyer's law, which correlates the test load and the resultant indentation size using a simple power law,[1,2]

$$P_{max} = Ah_c^n \quad (4)$$

where A and n are constants that can be derived directly from curve fitting of the experimental data. Especially, the exponent n, sometimes referred to as the Meyer's index, is usually considered as a measure of the ISE. Compared with the definition of the apparent hardness, Eq. (1), one can see that no ISE would be observed when $n = 2$.

The nanoindentation data for the materials examined in the present study are now plotted in an $\ln P_{max} - \ln h_c$ scale in Fig. 3. Each set of the data shows an excellent linear relationship, implying that the traditional Meyer's law is suitable for describing the nanoindentation data. Through linear regression analyses, the best-fit values of the parameters A and n were obtained and the results are summarized in Table 1.

4.2. Hays–Kendall approach

When examining the ISE in the Knoop hardness testing of a number of metals, Hays and Kendall[4] advanced a concept that there exists a minimum level of the applied test load, W, named the test-specimen resistance, below which permanent deformation due to

Table 1
Best-fit results of the parameters in Eqs. (4) and (5)

Material	Eq. (4)			Eq. (5)		
	n	A (mN/nm^n)	r	W (mN)	A_1 (mN/nm^2)	r
Glass	1.965	2.00×10^{-4}	0.99974	1.28	1.60×10^{-4}	0.99994
TZP	1.954	4.85×10^{-4}	0.99995	4.92	4.56×10^{-4}	0.99991
Si_3N_4	1.915	8.44×10^{-4}	0.99989	2.80	4.77×10^{-4}	0.99997

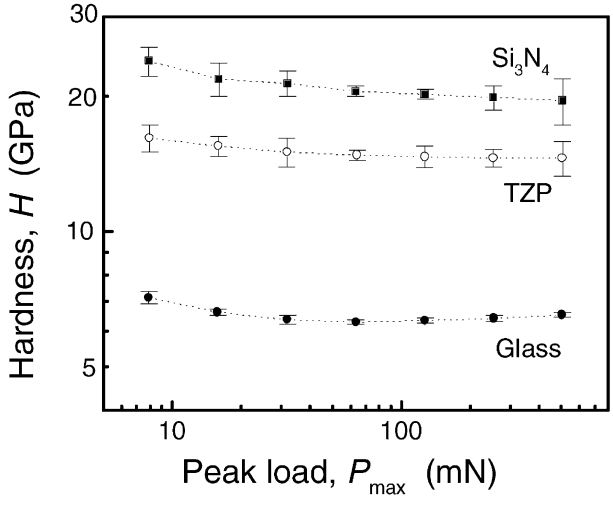

Fig. 2. Variation of nanoindentation hardness with the peak load for the test materials.

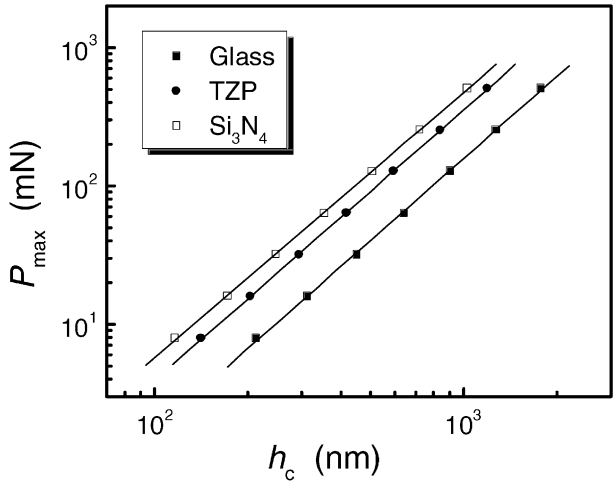

Fig. 3. Dependency of $\ln P_{max}$ on $\ln h_c$ according to the Meyer's law for the test materials.

indentation does not initiate, but only elastic deformation occurs. They introduced an effective indentation load, $P_{eff} = P_{max} - W$, and proposed the following relationship,

$$P_{max} - W = A_1 h_c^2 \quad (5)$$

where W and A_1 are constants independent of the test load for a given material.

Eq. (5) predicts that a plot of P_{max} versus h_c^2 would yield a straight line. Such plots for the materials considered in the present study are shown in Fig. 4 and Table 1 lists the best-fit results of the P_{max}–h_c^2 plots shown in Fig. 4. As can be seen, the correlation coefficient, r, of each plot is very high, > 0.999, implying that Eq. (5) provides a satisfactory description of the nanoindentation data for the test materials.

4.3. Elastic recovery model

In microhardness tests, the indentation size is measured after the indenter is removed from the specimen surface. Note that the elastic recovery would occur in the vicinity of the remaining indentation impression after the indenter is removed so that the indentation size would shorten to a certain degree.[14] Considering this effect, Tarkanian et al.[5] suggested that the measured indentation size should be corrected with a revised term in order to obtain the true hardness, i.e.,

$$H_0 = k\frac{P}{(d + d_0)^2} \quad (6)$$

where d_0 is the correction in the indentation size d due to the elastic recovery and k is a constant dependent on the indenter geometry.

Although the load–displacement curves such as those shown in Fig. 1 are recorded during indentation test, the indentation size, h_c, used for the hardness calculation can also be considered as the size measured after the elastic recovery occurs, see Eq. (3). Furthermore, several authors have pointed out that, for calculating the hardness from the recorded indentation tests such as the nanoindentation, similar correction in indentation size should be considered because of the elastic recovery associated with new bands of plastic deformation[15] and/or the blunting of the indenter tip.[16] Thus it is necessary to check if Eq. (6) is suitable for describing the nanoindentation data obtained for ceramics.

To analyze the nanoindentation data, Eq. (6) may be rewritten in the form

$$P_{max}^{1/2} = \chi^{1/2} h_c + \chi^{1/2} h_0 \quad (7)$$

where h_0 is the correction in h_c and $\chi = H_0/k$ is a constant related to the true hardness. Eq. (7) allows to determine h_0 and χ from the plots of $P_{max}^{1/2}$ against h_c. Fig. 5 shows such plots for the test materials while the best-fit values of the parameters χ and h_0 are listed in Table 2. For each material, the correlation coefficient of the $P_{max}^{1/2}$ against h_c plot is very high.

There are two ways to calculate the true hardness based on the elastic recovery model. One is to directly use Eq. (6) and the other is to use $\chi = H_0/k$. The calculated results are listed in Table 2 and shown in Fig. 6. In Table 2 and Fig. 6, $(H_0)_1$ denotes the true hardness calculated with Eq. (6) using the best fit-value of h_0 and $(H_0)_2$ the true hardness calculated from $\chi = H_0/k$ using $k = 1/24.5$ for nanoindentation test.

Table 2
Best-fit results of the parameters in Eq. (7)

Material	χ (mN/nm^2)	h_0 (nm)	r	$(H_0)_1$ (GPa)	$(H_0)_2$ (GPa)
Glass	1.58×10^{-4}	−0.19	0.99990	6.53±0.29	6.45
TZP	3.51×10^{-4}	7.34	1.00000	14.36±0.11	14.33
Si_3N_4	4.67×10^{-4}	13.56	1.00000	19.06±0.15	19.06

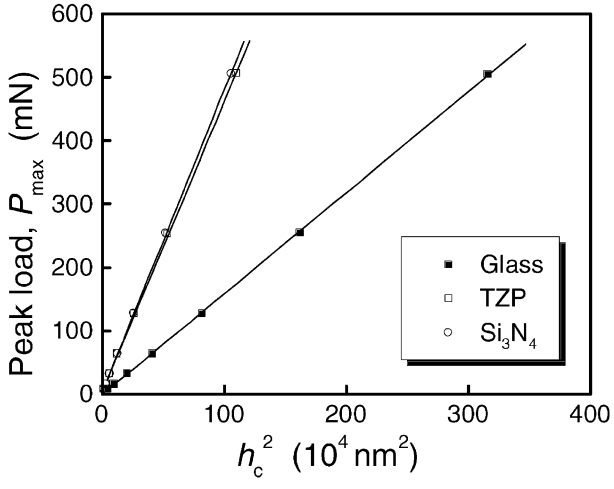

Fig. 4. Plots of P_{max} versus h_c^2 according to the Hays–Kendall approach.

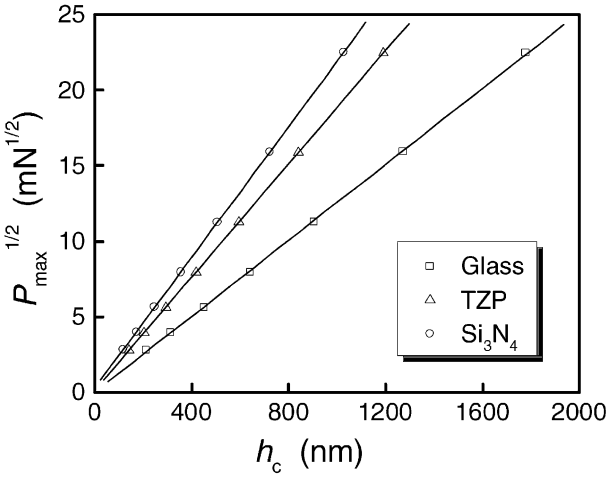

Fig. 5. Plots of $P_{max}^{1/2}$ against h_c for the test materials.

4.4. Proportional specimen resistance model

Proportional specimen resistance (PSR) model was proposed by Li and Bradt.[8] This model can be considered as a modified form of the Hays–Kendall approach. In this model, the test-specimen resistance to permanent deformation is assumed not to be a constant, but increase linearly with the indentation size, i.e.,

$$W = a_1 h_c \tag{8}$$

To a first approximation, the form of Eq. (8) can be considered to be similar to the elastic resistance of a spring with the opposite sign to the applied test load. Then, the effective indentation load and the indentation dimension can be related as:

$$P_{eff} = P_{max} - W = P_{max} - a_1 h_c = a_2 h_c^2 \tag{9}$$

where a_1 and a_2 are constants for a given material. According to the analysis of Li and Bradt,[8] the parameters a_1 and a_2 can be related to the elastic and the plastic properties of the test material, respectively. Especially, a_2 was suggested to be a measure of the so-called *true hardness*, i.e., load-independent hardness, H_0. For the nanoindentation test with a Berkovich indenter, H_0 can be determined directly from a_2 with

$$H_0 = \frac{P_{eff}}{24.5 h_c^2} = \frac{P_{max} - a_1 h_c}{24.5 h_c^2} = \frac{a_2}{24.5} \tag{10}$$

Eq. (9) can be rearranged as

$$\frac{P_{max}}{h_c} = a_1 + a_2 h_c \tag{11}$$

which enables to determine both a_1 and a_2 from the plot of P_{max}/h_c against h_c.

An alternative explanation for the physical meaning of Eq. (11) was proposed by Fröhlich et al.[6] based on an energy-balance analysis. A detailed description of the energy balance analysis was given by Quinn and Quinn recently.[7] According to the energy balance consideration, the parameters a_1 and a_2 in Eq. (11) are related to the energies dissipated for creating a new surface of a unit area and for producing the permanent deformation of a unit volume, respectively. Also, a_2 is a measure of the true hardness.

Plots of P_{max}/h_c versus h_c were drawn for all the materials examined in the present study and are now shown in Fig. 7. Analysis of the experimental data according to Eq. (11) yields the best-fit values of a_1 and a_2 for each material and the results are listed in Table 3.

To evaluate the applicability of the PSR model in analyzing the ISE, two sets of H_0-values, i.e., $(H_0)_1 = (P_{max} \ a_1 h_c)/(24.5 h_c^2)$ and $(H_0)_2 = a_2/24.5$, were calculated for each material. The results are given in Table 3 and Fig. 8. In Fig. 8, $(H_0)_1$-values are plotted as

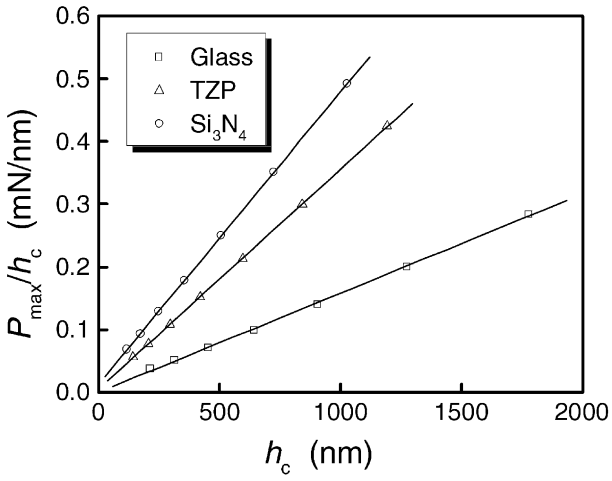

Fig. 7. Plots of P_{max}/h_c versus h_c according to the PSR model.

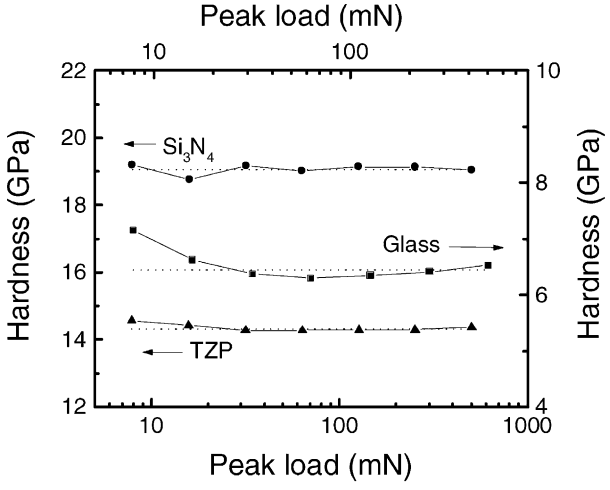

Fig. 6. True hardness numbers determined based on the elastic recovery model as functions of the peak load. Symbols: $(H_0)_1$; dotted lines: $(H_0)_2$.

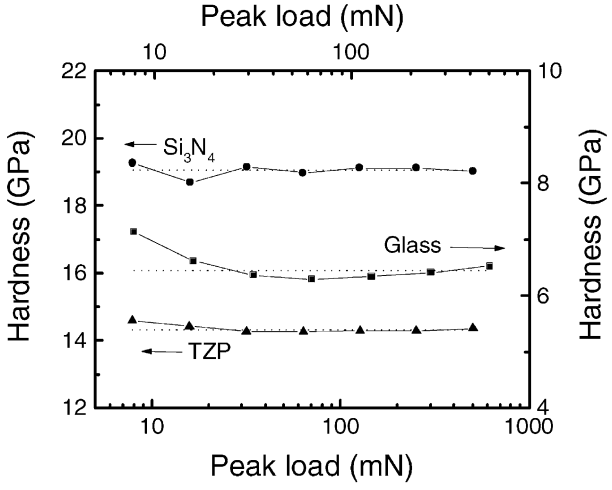

Fig. 8. True hardness numbers determined based on the PSR model as functions of the peak load. Symbols: $(H_0)_1$; dotted lines: $(H_0)_2$.

symbols and $(H_0)_2$-values as dotted lines. Clearly, the two sets of H_0-data are in good agreement with each other although there is a somewhat large scatter in the calculated $(H_0)_1$-values for each material.

4.5. The modified PSR model

When examining the load-dependence of the microhardness of some silicon nitride based ceramics measured in a wide load range, Gong et al.[17] found that the resultant P/d–d (where d is half-length of the Vickers indentation) curves exhibit significant nonlinearity and argued that the PSR model mentioned above may only be used to represent the experimental data measured in a narrower range of applied loads. By considering the effect of the machining-induced plastically deformed surface on the hardness measurements, Gong et al. suggested that the PSR model should be modified as[9]

$$P_{\max} = a_0 + a_1 h_c + a_2 h_c^2 \quad (12)$$

where a_0 is a constant related to the surface residual stresses associated with the surface machining and polishing and a_1 and a_2 are the same parameters as those in Eq. (11).

An equation with the same form as Eq. (12) was also deduced based on a modified energy-balance analysis [18]. Compared with the equation deduced based on the traditional energy-balance consideration, Eq. (11), a constant a_0-term was introduced in Eq. 12 and this term was suggested to be related to the experimental errors associated with the optical resolution of the objective lens used and/or the sensitivity of the load cell.

The applications of Eq. (12) to all the materials studied in this work are now illustrated in Fig. 9. The solid lines in these plots are obtained by a conventional polynomial regression according to Eq. (12). The best-fit values of the parameters included in Eq. (12) for each material are listed in Table 4.

Similar to the PSR model, the modified PSR model also provides two different ways for the calculation of the true-hardness, i.e., $(H_0)_1 = (P_{\max} - a_0 - a_1 h_c)/(24.5 h_c^2)$ and $(H_0)_2 = a_2/24.5$. The calculated $(H_0)_1$ and $(H_0)_2$ are listed in Table 4 and shown in Fig. 10.

5. Discussion

Five empirical or semi-empirical equations were employed to describe the nanoindentation data obtained for glass and ceramics. It was proved that each of them may provide satisfactory description for the relationship between peak load and the resultant indentation size. This experimental finding is similar to those obtained when analyzing the microhardness data.[8–12]

Table 3
Best-fit results of the parameters in Eq. (11)

Material	a_1 (mN/nm)	a_2 (mN/nm^2)	r	$(H_0)_1$ (GPa)	$(H_0)_2$ (GPa)
Glass	-0.22×10^{-4}	1.58×10^{-4}	0.99959	6.53±0.29	6.45
TZP	0.0053	3.51×10^{-4}	0.99998	14.35±0.12	14.33
Si_3N_4	0.0133	4.67×10^{-4}	0.99998	19.04±0.18	19.06

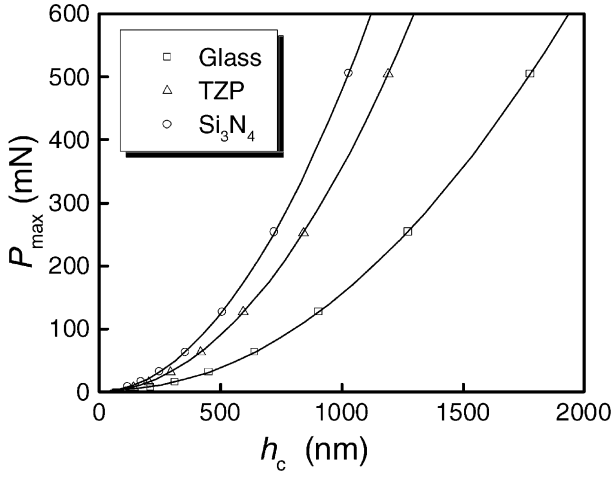

Fig. 9. Indentation size versus the peak load for test materials.

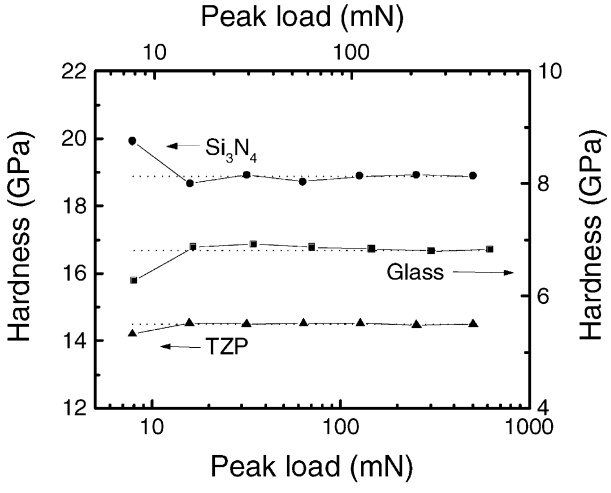

Fig. 10. True hardness numbers determined based on the modified PSR model as functions of the peak load. Symbols: $(H_0)_1$; dotted lines: $(H_0)_2$.

However, the applicabilities of these empirical or semi-empirical equations to the description of the ISE observed in nanohardness tests should be discussed further based on the physical meanings of the parameters included in each equation.

Meyer's law is the first attempt to quantify the ISE. Several studies have been conducted to explore the relation between the two parameters, n and A, included in Meyer' law [Eq. (4)]. For example, Sargent and Page[19] considered several "n value versus ln A" relationships in an attempt to ascertain any possible microstructural effects on those power law parameters. They found that, for polycrystalline ceramics, lower n values are generally associated with higher ln A values. A similar tendency was also observed in the present study, see Table 1. However, it should be pointed out that the knowledge of the correlation between n and A seems to be of little significance for understanding the ISE, because our previous study has found that the best-fit value of the Meyer's law coefficient A depends on the unit system used for recording the experimental data and completely different trends of n versus A may be observed in different unit systems.[20] Previous studies also tried to relate the Meyer's index, n, to the microstructural features. In a study on the Vickers hardness testing for hot-pressed Si_3N_4-based ceramics, Babini et al.[21] found that the n value increases as grain size increases. A more recent study[10] showed that the microhardness of TiCN-based cermets increases with increasing load and, in this case, n decreases with the increasing grain size. However, knowledge of the generality of the correlation between n and grain size is still lacking. In fact, previous studies[8,9] have pointed out that, as a pure empirical equation, Meyer's law cannot provide any knowledge of the origin of ISE.

One important parameter which can be extracted from the analysis of the experimental data according to the Hays–Kendall approach is W, the minimum test load under which the material would exhibit a permanent deformation. It was generally reported[8,9,12] that the W-values deduced from the microhardness tests are too large to be acceptable. In the present study, similar conclusions can also be obtained. For example, the best-fit value of W for TZP is 4.92 mN (Table 1). To check if this W-value is acceptable, additional nanoindentation test was conducted for TZP under a peak load of 1 mN and the resultant load–displacement curve is shown in Fig. 11. Clearly, the loading portion and the unloading portion in this plot are well separated, indicating that a permanent deformation occurred during indentation. This means that the minimum load necessary to initiate permanent deformation for TZP is lower than 1 mN. Therefore, one can conclude that the Hays–Kendall approach is not suitable for describing the nanoindentation data.

Indenter tip blunting effect has been considered as a main source for the errors in the determination of the penetration depth during nanoindentation tests and it is usually suggested that the real penetration depth should be somewhat larger than that deduced by analyzing the load–penetration curve.[16,22] On the other hand, elastic recovery occurring after indenter is removed would result in a shorten in the indentation size. Therefore, the correction factor h_0 in Eq. (7) should have a positive value. However, a negative value of h_0 was observed for soda-lime glass (Table 2). Furthermore, the h_0-value for Si_3N_4, 13.56, seems to be too large to be accepted. Therefore, the ISE shown in Fig. 2 cannot be explained using the elastic recovery model. At least, the error in indentation size due to indenter tip blunting effect and the elastic recovery after indentation are not the only source of the ISE observed in the present study.

As a modified form of the Hays–Kendall approach, the PSR model treats the specimen's resistance to permanent deformation as a function of indentation size, rather than a constant. Li and co-workers[8,23,24]

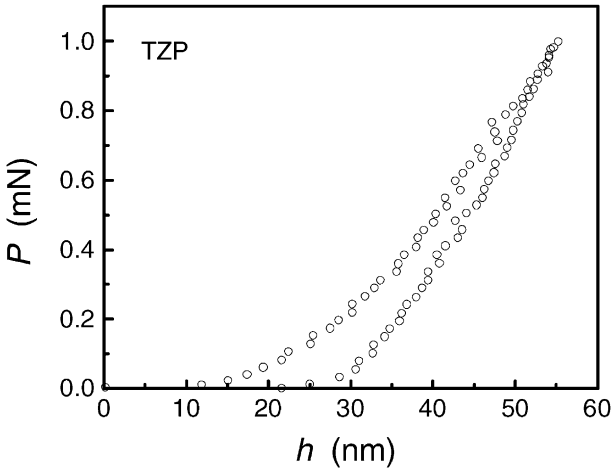

Fig. 11. Load–displacement curve measured on TZP under a peak load of 1 mN. Note that the loading portion and the unloading portion are well separated, indicating that a permanent deformation occurs during indentation.

Table 4
Best-fit results of the parameters in Eq. (12)

Material	a_0 (mN)	a_1 (mN/nm)	a_2 (mN/nm^2)	r	$(H_0)_1$ (GPa)	$(H_0)_2$ (GPa)
Glass	4.28	−0.016	1.67×10^{-4}	0.99999	6.77±0.22	6.82
TZP	0.84	7.24×10^{-4}	3.55×10^{-4}	1.00000	14.46±0.12	14.49
Si_3N_4	−0.71	0.017	4.63×10^{-4}	1.00000	18.98±0.42	18.88

concluded that this model may provide a satisfactory explanation for the origin of ISE in microhardness tests for various materials. As can be seen from Table 3, similar conclusion can also be obtained in the present study when analyzing the nanoindentation data for TZP and Si_3N_4 with the PSR model. However, when applying this model to soda-lime glass, the PSR model yielded a negative a_1-value and, clearly, this negative value, although being very small, cannot be explained based on the physical meaning of the parameter a_1 proposed by Li and Bradt.[8] Similar phenomenon was also observed when analyzing the nanoindentation data according to the modified PSR model. As previously pointed out, the parameter a_1 in the modified PSR model has the same physical meaning as that in the PSR model.[9] Therefore, the negative a_1-value listed in Table 4 implies that the modified PSR model cannot provide a satisfactory explanation for the ISE observed for soda-lime glass.

There have been several studies[10–12,25] concerning the applicability of the modified PSR model to describing the ISE. It was found that, although a much high correlation coefficient can be obtained when analyzing the indentation data according to Eq. (12), in some cases, the resultant best-fit values of the parameters included in this equation cannot be explained satisfactorily based on the modified PSR model. Noting that Eq. (12) can also be deduced by combining the experimental errors into the energy-balance consideration,[18] we can speculate that Eq. (12) may concern various factors which contribute to the ISE. Therefore, any attempt to relate the parameters a_0 and/or a_1 to a unique factor may be unreasonable and inappropriate.

Based on the above analyses, one can conclude that the ISE observed in nanoindentation tests is a rather complex phenomenon and cannot be explained based on a unique mechanism. Although two possible explanations for Eq. (12) have been proposed, there is reason to believe that the physical meanings of the parameters included in this equation seem to be more complex than those proposed previously.

The main goal of describing the ISE with an empirical or semi-empirical equation is to find a way to determine the so-called true hardness for material characterization. As can be seen from Tables 2, 3 and 4, for each material, the true hardness values determined based on different models are in good agreement with each other. This seems to say that, although there still exist some obstacles in understanding origin of the ISE based on each model, a comparable true hardness may be obtained. In fact, the consistency in the resultant true hardness values can be attributed to the similarity between Eqs. (6), (11) and (12). Clearly, these three equations may be considered as truncated forms of the polynomial series representation of the applied load which was applied by Bückle[26] to analyze the ISE,

$$P_{\max} = a_0 + a_1 h_c + a_2 h_c^2 + \cdots a_n h_c^n \quad (13)$$

Especially, Eqs. (6) and (12) have the exactly same form despite of the difference in the explanations of the physical meanings. From a viewpoint of statistics, it is not surprising that the a_2-values, i.e., the measure of the true hardness, are nearly the same for each model when analyzing the experimental data measured in a relatively narrow load range.

6. Conclusions

The load-dependences of the nanoindentation hardness for soda-lime glass, TZP and Si_3N_4 were examined in the present study. Particular emphasis was paid to the applicabilities of some previously proposed empirical or semi-empirical equations to the description of the nanoindentation data. The following conclusions were deduced:

1. Meyer's law was proved to be sufficient for the description of the experimental data. However, no useful knowledge of the origin of the observed ISE may be provided based on this empirical equation.
2. The minimum load required for initiating the permanent deformation predicted by the Hays–Kendall approach was too large to be acceptable, invalidating the applicability of this approach in analyzing the ISE.
3. The PSR model can be used to analyze the ISE observed in glass and Si_3N_4 but failed in analyzing the reversed ISE observed in TZP.
4. The elastic recovery model yielded unreasonable values for the indentation size correction factor, d_0, implying that errors in indentation size measurements due to elastic recovery and/or indenter tip blunting are not the only source of the ISE observed in the present study.
5. The modified PSR is suitable for describing the experimental data. However, the physical meanings of the parameters included in this model seem to be more complex than those proposed previously.
6. The values of the true hardness, H_0, were determined based on the PSR model, the elastic recovery model and the modified PSR model, respectively. The resultant H_0-values were found to be independent of the model selected. This phenomenon was attributed to the similarity between the equations used in these three models.

Acknowledgements

The authors would like to thank Mrs. Yang Gao for her assistance in the nanoindentation tests. The authors

would also like to thank the critical comments and suggestions made by the reviewer.

References

1. Tabor, D., *The Hardness of Metals*. Oxford University Press, Oxford, UK, 1951.
2. Mott, B. W., *Microindentation Hardness Testing*. Butterworths, London, 1956.
3. Clinton, D. J. and Morrell, R., Hardness testing of ceramic materials. *Mater. Chem. Phys.*, 1987, **17**, 461–473.
4. Hays, C. and Kendall, E. G., An analysis of Knoop microhardness. *Metall.*, 1973, **6**, 275–282.
5. Tarkanian, M. L., Neumann, J. P. and Raymond, L., Determination of the temperature dependence of {100} and {112} slip in tungsten from Knoop hardness measurements. In *The Science of Hardness Testing and Its Research Applications*, ed. J. H. Westbrook and H. Conrad. American Society for Metals, Metal Park, OH, 1973, pp. 187–198.
6. Fröhlich, F., Grau, P. and Grellmann, W., Performance and analysis of recording microhardness tests. *Phys. Status Solidi*, 1977, **42**, 79–89.
7. Quinn, J. B. and Quinn, G. D., Indentation brittle of ceramics: a fresh approach. *J. Mater. Sci.*, 1997, **32**, 4331–4346.
8. Li, H. and Bradt, R. C., The microhardness indentation load/size effect in rutile and cassiterite single crystals. *J. Mater. Sci.*, 1993, **28**, 917–926.
9. Gong, J. H., Wu, J. J. and Guan, Z. D., Examination of the indentation size effect in low-load Vickers hardness testing of ceramics. *J. Eur. Ceram. Soc.*, 1999, **19**, 2625–2631.
10. Gong, J. H., Miao, H. Z., Zhao, Z. and Guan, Z. D., Load-dependence of the measured hardness of Ti(C,N)-based cermets. *Mater. Sci. Eng.*, 2001, **A303**, 179–186.
11. Kim, H. and Kim, T., Measurement of hardness on traditional ceramics. *J. Eur. Ceram. Soc.*, 2002, **22**, 1437–1445.
12. Sangwal, K., Surowska, B. and Blaziak, P., Analysis of the indentation size effect in the microhardness measurement of some cobalt-based alloys. *Mater. Chem. Phys.*, 2002, **77**, 511–520.
13. Oliver, W. C. and Pharr, G. M., An improved technique for determining hardness and elastic modulus using load and displacement sensing indentation experiments. *J. Mater. Res.*, 1992, **7**, 1564–1583.
14. Lawn, B. R. and Howes, V. R., Elastic recovery at hardness indentations. *J. Mater. Sci.*, 1981, **16**, 2745–2752.
15. Weiss, H. J., On deriving Vickers hardness from penetration depth. *Phys. Status Solidi*, 1987, **99**, 491–501.
16. Bull, S. J., Page, T. F. and Yoffe, E. H., An explanation of the indentation size effect in ceramics. *Phil. Mag. Lett.*, 1989, **59**, 281–288.
17. Gong, J. H., Wu, J. J. and Guam, Z. D., Description of the indentation size effect in hot-pressed silicon-nitride-based ceramics. *J. Mater. Sci. Lett.*, 1998, **17**, 473–475.
18. Gong, J. H. and Li, Y., An energy-balance analysis for the size effect in low-load hardness testing. *J. Mater. Sci.*, 2000, **35**, 209–213.
19. Sargent, P. M. and Page, T. F., The influence on the microhardness of ceramic materials. *Proc. Brit. Ceram. Soc.*, 1978, **26**, 209–224.
20. Gong, J. H., Zhao, Z., Guan, Z. D. and Miao, H. Z., Load-dependence of Knoop hardness of Al_2O_3-TiC composites. *J. Eur. Ceram. Soc.*, 2000, **20**, 1895–1900.
21. Babini, G. N., Bellosi, A. and Galassi, C., Characterization of hot-pressed silicon nitride based materials by microhardness measurements. *J. Mater. Sci.*, 1987, **22**, 1687–1693.
22. Martin, M. and Troyon, M., Fundamental relations used in nanoindentation: critical examination based on experimental measurements. *J. Mater. Res.*, 2002, **17**, 2227–2234.
23. Li, H. and Bradt, R. C., The indentation load/size effect and the measurements of the hardness of vitreous silica. *J. Non-Cryst. Solids*, 1992, **146**, 197–212.
24. Li, H., Ghosh, A., Han, Y. H. and Bradt, R. C., The frictional component of the indentation size effect in low load microhardness testing. *J. Mater. Res.*, 1993, **8**, 1028–1032.
25. Gong, J. H., Comment on "Measurement of hardness on traditional ceramics". *J. Eur. Ceram. Soc.*, 2003, **23**, 1769–1772.
26. Bückle, H., *Mikrohärteprüfung*. Berliner Union Verlag, Stuttgart, 1965.